Review on Key Technologies and Development of Magnetic Coupling Resonant-Dynamic Wireless Power Transfer for Unmanned Ground Vehicles

Feifan Xu, Shuguang Wei, Dong Yuan and Jiaqi Li *

Department of Control Engineering, Army Academy of Armored Forces, Beijing 100072, China;
extraordinaryxu@163.com (F.X.)
* Correspondence: lijiaqi8643@163.com

Abstract: With the fast development of magnetic coupling resonant-dynamic wireless power transfer (MCR-DWPT), it is more likely that high-efficiency wireless charging between unmanned ground vehicles (UGVs) will be practically realized, especially in desolate places that are far away from a city center or charging depot and always experiencing large load fluctuations, varying operating conditions, and complex working targets. Based on this, the wireless charging of UGVs demands higher reliability and efficiency. This paper reviews the MCR-DWPT system of UGVs, and the basic structure and key technologies are introduced. Then, the key technologies, which include the coupling device design, compensation topology design, and system control strategy, are discussed in detail. After that, by considering the current research, the main challenges of the MCR-DWPT of UGVs are investigated and its developing prospects are explored.

Keywords: unmanned ground vehicle; magnetic coupling resonant-dynamic wireless power transfer; coupling device; compensation topology; control strategy

1. Introduction

With the development of artificial intelligence and automatic control technology, outstanding achievements regarding electric drives, electromagnetic weapons, and protection have increasingly been applied in unmanned ground vehicles (UGVs), which have an urgent demand for a reliable means of power transmission [1]. Based on the vehicles' integrated power systems, UGVs are likely to realize information interaction and power sharing [2].

Magnetic coupling resonant-dynamic wireless power transfer (MCR-DWPT) is a type of wireless power transfer (WPT) technology that is able to transmit and receive power wirelessly with higher transmission and power efficiency at the meter level. As a non-contact power transmission technology realized by the near-field coupling of an electromagnetic field, MCR-DWPT has the ability to effectively improve the drawbacks existing in traditional wired power transmission, including wire aging, plug damage, electric arcs when plugging and unplugging, potential electric accidents, high maintenance costs, and weak environmental adaptability. Compared to static wireless charging at a specified position, MCR-DWPT technology can realize "charging while moving", which meets the requirements of the UGV charging system [3].

Currently, MCR-DWPT technology has made outstanding progress in electric vehicles [4], consumer electronics [5], medical devices [6], wireless sensor networks [7,8], and other civilian fields [9]. For MCR-DWPT of UGVs, most studies focus on the operating environment of city roads and factory transportation with the purpose of realizing MCR-DWPT of UGVs with transmitters buried in the ground. In desolate places of operation such as hillside, forest, and desert, there has been insignificant research progress in MCR-DWPT

between UGVs due to the transmission power level, operating conditions, and working environment.

In order to promote MCR-DWPT of UGVs in desolate operating environments, the literature about MCR-DWPT in the last five years has been referred to, and papers of great reference and application value for the key technologies of MCR-DWPT have been quoted. Based on this, the paper first introduces the research background of MCR-DWPT and focuses on the specific requirements of UGVs operating in desolate places. Then, the key technologies of the MCR-DWPT system, such as the coupling device design, compensation topology design, and system control strategy, are reviewed in detail. Finally, the main challenges of the MCR-DWPT of UGVs are summarized, which provides a reference for the future research of the MCR-DWPT of UGVs in desolate environments.

2. MCR-DWPT of UGVs

2.1. Basic Structure of MCR-DWPT of UGVs

Figure 1 shows a general structure of the MCR-DWPT of UGVs. There is a type-I platform, which acts as a power supplier, while a type-II platform acts as a power receiver. The DC networks of these two platforms, U_I and U_{II}, are connected by a subsystem that realizes the WPT between the type-I and type-II platforms. The transmitter of the MCR-DWPT system is placed on the type-I platform, while the receiver is placed on the type-II platform. The high-frequency inverter of the transmitter inverts the DC of the type-I platform network into high-frequency AC. After reactive power compensation and power transmission in the electromagnetic field of the WPT subsystem, the aforementioned AC is rectified into DC by the high-frequency rectification circuit at the receiver and then transmitted into the type-II platform network. Finally, the WPT between the two platforms is realized.
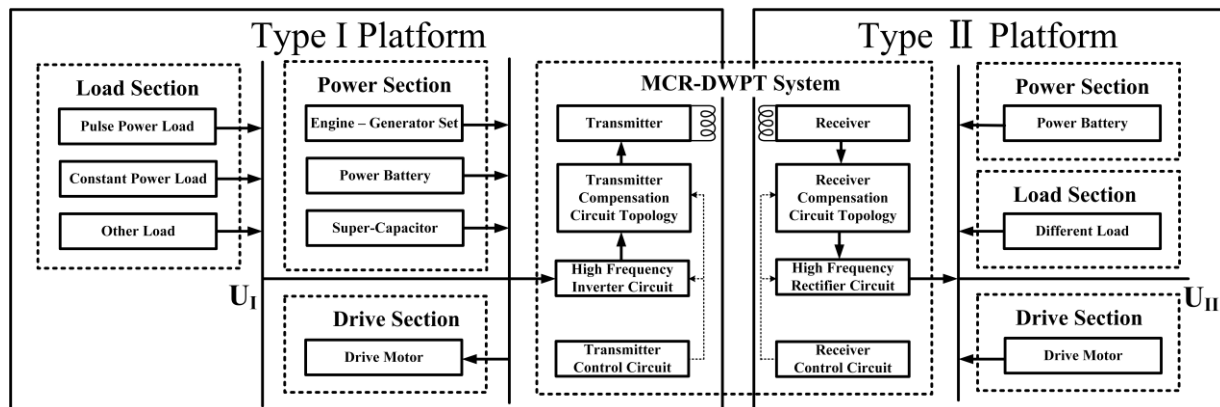
Figure 1. General structure of MCR-DWPT of UGVs.

2.2. Characteristics of MCR-DWPT of UGVs

Although many research results have been achieved in the civilian field of MCR-DWPT, such as in urban electric vehicles (EVs) [10], unmanned aerial vehicles (UAVs) [11], and so on, the characteristics of the UGV MCR-DWPT system are different because of the difficult operating conditions, which are listed below:

1. Random relative position and fluctuating load.

Different from urban EVs, the movement of UGVs in desolate places is more random, which leads to a random relative position between UGVs and an inconstant coupling coefficient. Moreover, the various working conditions cause changes in the load characteristics and the fluctuation of circuit parameters [12]. Therefore, a coupling device with stronger anti-offset performance, compensation topologies with better adaptability, and control strategies with better reliability are essential.

2. Complex working conditions and difficult desolate situations.

The working conditions of UGVs are selected by considering the driving environments and situations. During normal operation, the transmission efficiency is of particular importance inside an MCR-DWPT system. However, the transmission power is mostly considered during off-road driving. Therefore, the transmission characteristics of the MCR-DWPT system have to be accurately analyzed to maintain a high transmission power and efficiency under various operating and driving conditions [2].

3.　　Harsh environments and high requirements for reliability.

The MCR-DWPT system of UGVs has higher requirements for reliability, safety, and electromagnetic compatibility. More importantly, it is necessary to maintain the transmitter and the receiver of the MCR-DWPT system with a normal working status, regardless of communication. Furthermore, the wireless charging should be able to be automatically stopped for safety reasons in the case of an unknown object existing between the transmitter and the receiver. Finally, when multiple targets are being charged, the MCR-DWPT system should be able to distribute the charging power to several objects to improve the overall charging efficiency [13].

3. Key Technologies of MCR-DWPT of UGVs

The key technologies of MCR-DWPT mainly include the coupling device design, compensation topology design, and system control strategy, which are introduced below.

3.1. Optimization Design of Coupling Devices

For MCR-DWPT systems of UGVs, different structures of coupling device have different anti-offset performance. Many scholars have designed various structures of coupling devices to improve the device performance under different operating conditions [14–17]. In this section, the impact of spatial motion on WPT is analyzed. Then, the main research results of the above structures are summarized and classified to provide ideas for the future design of coupling devices.

3.1.1. Impact of Spatial Motion on WPT

In the case of two coupling devices, there are mainly four types of spatial motion modes in WPT, which are axial offset, horizontal offset, horizontal turnover, and horizontal rotation along the symmetry axis, which are shown in Figure 2.
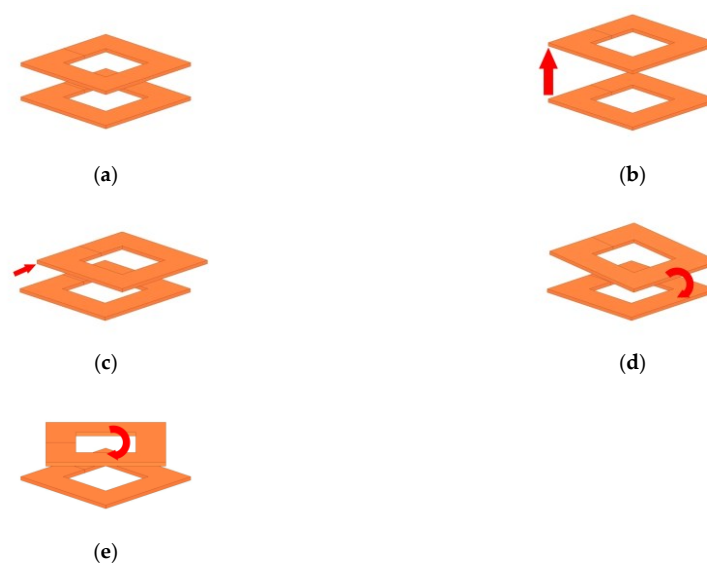
Figure 2. Spatial motion modes of coupling devices: (**a**) reference state; (**b**) axial offset; (**c**) horizontal offset; (**d**) horizontal turnover; (**e**) horizontal rotation along the symmetry axis.

The effects of the coupling device spatial motion are analyzed as follows.

When an axial offset occurs, the flux density between the devices decreases with an increase in the distance between them, and the coupling coefficient and transmission efficiency of the WPT system decrease gradually.

When a horizontal offset occurs, in terms of the flux density between the coupling devices, the coupling coefficient, and the transmission efficiency of the WPT system, they either remain constant or slightly increase within a certain offset range according to the different structures of the coupling devices. When the offset distance is too large, the flux density between the coupling devices gradually weakens with an increase in the offset distance; therefore, the coupling coefficient and transmission efficiency of the WPT devices gradually decrease.

When one coupling device turns horizontally, it creates an angle with the other coupling device. In this case, there are two situations, including the planar coupling device and the spatial coupling device. For the planar coupling device, the flux density between the coupling devices is gradually weakened with an increase in the turning angle so that the coupling coefficient and the transmission efficiency of the WPT system are gradually reduced [14]. For the spatial coupling device, since the original design was to improve the ability to resist angle offset, the flux density between most spatial coupling devices is not sensitive to a change in the flip angle, so there is a slight change in the coupling coefficient and the efficiency of the WPT system device [15].

When the coupling device rotates along the symmetry axis, different device structures have different magnetic field changes. For a disc-shaped coupling device, the magnetic field does not change because the disc-shaped coupling device rotates along the symmetry axis. Therefore, the coupling coefficient and the transmission efficiency of the WPT system do not change [16]. For a non-disk coupling device, the magnetic field between the coupling devices changes with the rotation of the device when the device rotates along the symmetry axis. The coupling coefficient and transmission efficiency of the WPT system also change accordingly [17].

In general, the practical spatial motion of the coupling device is always the integration of the above motions. As a result, coupling devices with different structures should be designed according to different operating conditions.

3.1.2. Structural Design of Coupling Devices

There are two main groupings of UGVs, which are the carrier type and the formation type [18]. According to the different groupings, the structure and anti-offset performance requirements of the coupling device are also different. The carrier type is mainly applicable to a situation where a large platform carries several small platforms to a target area and then unloads the small platforms to jointly operate. The coupling device is installed on the bottom of the small platform and on the floor in the cabin of the large platform to realize WPT during the carrying condition, but the coupling device is required to have good horizontal offset resistance. The formation type is mainly applicable to UGVs with similar vehicle types, so the coupling device is usually installed on one side of the vehicle's body. The coupling device is required not only for resisting horizontal offset but also for realizing the efficient transmission of power, especially when the distance and the horizontal flip angle between the transmitter and the receiver changes.

In order to minimize the size and improve the horizontal offset resistance of the WPT device, many studies have been conducted focusing on the receiver, which includes the circular pad (CP) [16], the double-D pad (DDP) [19], the bipolar pad (BPP) [20], and the double-D quadrature pad (DDQP) [21], as shown in Figure 3.

At the transmitter, it can be either the same as the receiver or adopt other structures, for instance, the long guide rail type or the segmented guide rail type, to improve the effective transmission area. Current research results of coupling devices are presented in Table 1. The Korean Academy of Science and Technology made a significant advance on the long guideway coupling device and consequently successfully proposed the E-type, U-type, W-type [22], I-type [23], S-type [24], and dq-type [25] device structures. There is

only one launch rail in the long guideway coupling device; therefore, the system voltage fluctuation is small and the control requirements are low, but the launch rail inductance and device resistance are large, the power loss is large, and the system transmission efficiency is low.
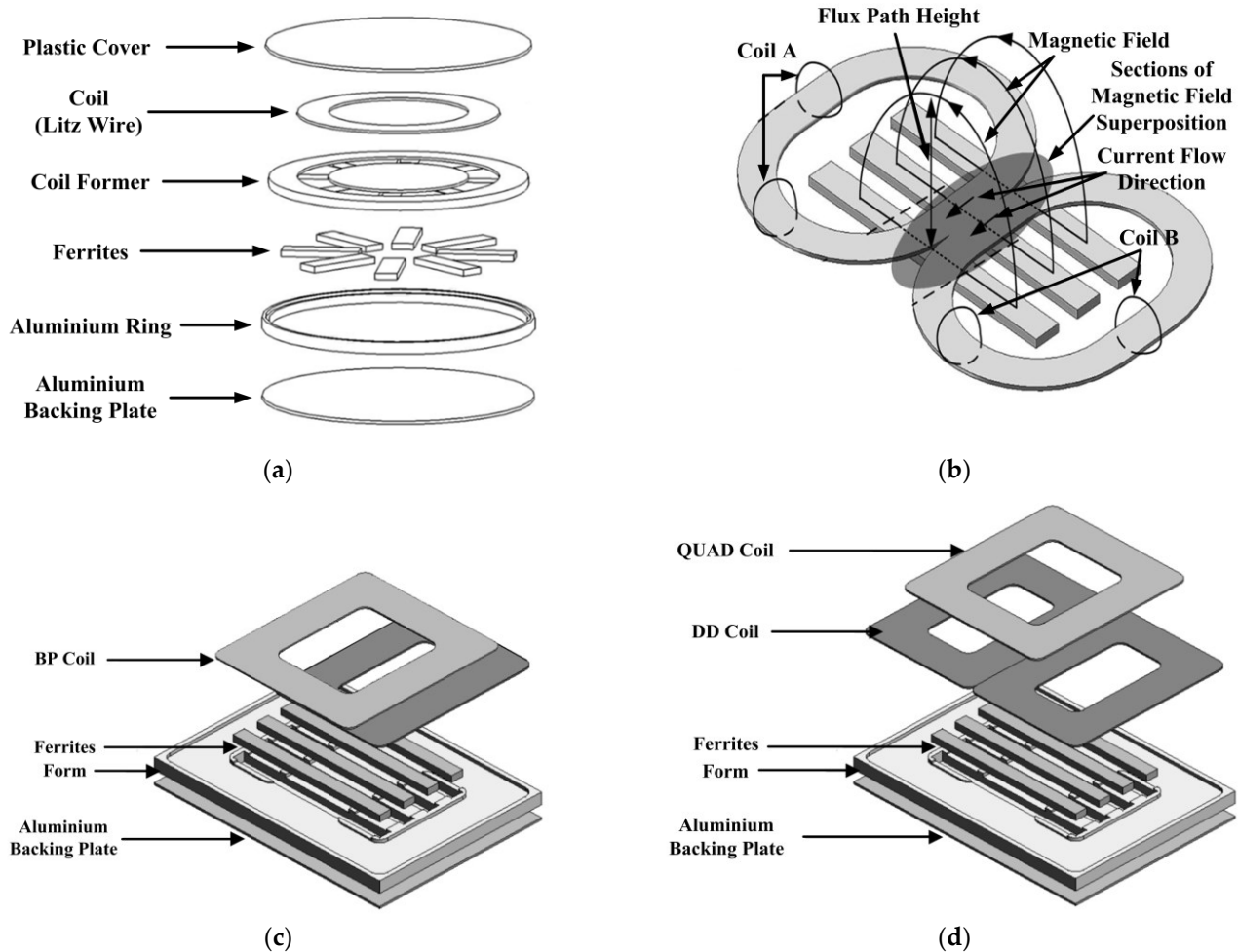
Figure 3. Four coupling device structures of the receiver prototype model: (**a**) CP; (**b**) DDP; (**c**) BBP; and (**d**) DDQP.

Table 1. Coupling devices for carrier-type grouping of UGVs [22–29].
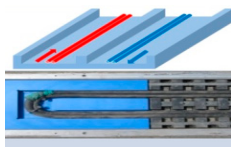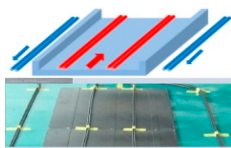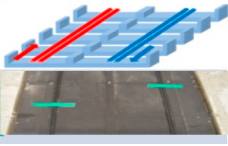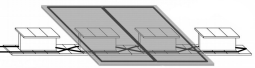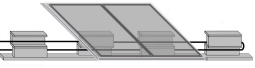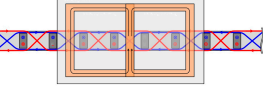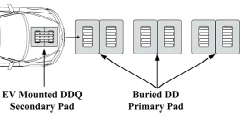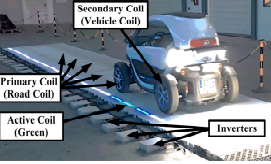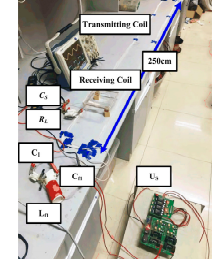
Classifications	Research institutions	Structures	Size	Performance
Long guide rail type	The Korean Academy of Science and Technology		E-type Width: 20 cm Gap: 1 cm	Power: 3 kW Efficiency: 80%
			U-type Width: 140 cm Gap: 17 cm	Power: 6 kW Efficiency: 72%

Table 1. *Cont.*

Classifications	Research institutions	Structures	Size	Performance
Long guide rail type	The Korean Academy of Science and Technology		W-type Width: 80 cm Gap: 20 cm	Power: 15 kW Efficiency: 83%
			I-type Width: 10 cm Gap: 20 cm	Power: 27 kW Efficiency: 74%
			S-type Width: 4 cm Gap: 20 cm	Power: 22 kW Efficiency: 91%
			dq-type Width: 80 cm Gap: 15 cm	Power: 0.2 kW Power fluctuation: about 11%
Segmented guide rail type	The University of Auckland		-	Power: about 10 kW Power fluctuation: about 25%
	Paris-Saclay University		Single device Side length: 455 mm	Power: 2.5 kW Efficiency: 92%
	China Electric Power Research Institute		Track trench Width: 200 mm Depth: 300 mm	Power: about 20 kW
	Southeast University		Transmitter Width: 150 mm Receiver Side Length: 150 mm	Power: 55W Efficiency: more than 85%

The University of Auckland [26], Paris-Saclay University [27], China Electric Power Research Institute [28], Southeast University [29], and other institutions have designed a variety of segmented guideway coupling devices. Compared to the long guide rail type, the structure of the segmented guide rail type coupling device is similar to that of the coupling device of static WPT. The system's efficiency is significantly improved by applying several independently working transmitters and dynamically controlling the output power of each transmitter. However, there are frequent voltage fluctuations at the receiver when switching transmitters, which strongly demands a precise control system for WPT.

There have been fewer studies on the WPT of formation-type UGVs. In [30], a mechanical structure was proposed to control the spatial position of the coupling device so that the transmitter and the receiver maintain alignment when moving in space, which improves the efficiency of WPT. However, the proposed mechanical structure has to consider extra factors, such as the structure's life and the control mode, which makes the whole system more complex. The prototype of the coupling device with a mechanical structure is shown in Figure 4. In [31], new coreless Tx coils with a conductive magnetic shield were proposed. They generate a planar rotating magnetic field to realize WPT between the transmitter and

the receiver in the case of relative horizontal reversal. However, the transmission power is small, and the efficiency is low.
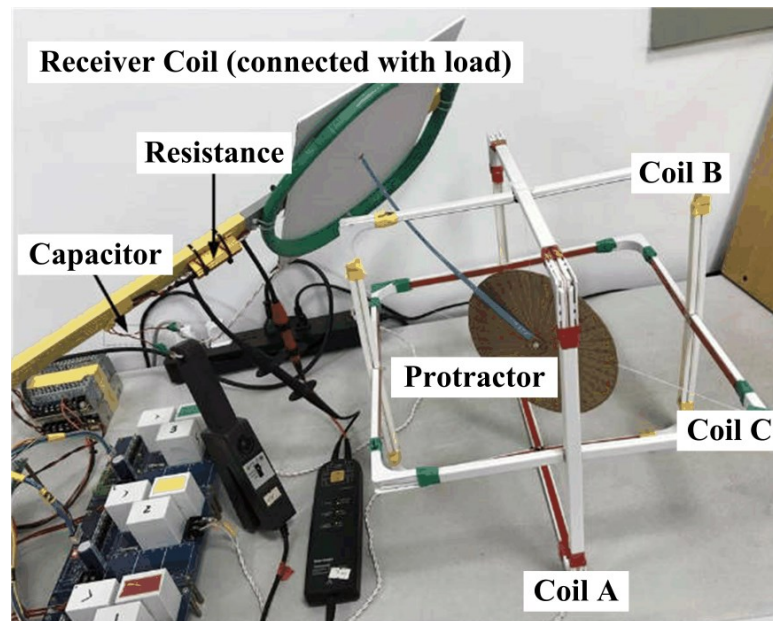
Figure 4. Prototype of the coupling device with mechanical structure.

3.2. Topology Design of the Compensation Circuit

The topological structure of the compensation circuit was designed to improve the instability caused by coupling coefficient changes and load fluctuations. Under dynamic conditions, system output characteristics such as a constant-voltage/current output, system power regulation, and efficiency maximization are maintained using an appropriate compensation topology. In addition, the compensation topology also helps to reduce the reactive power and improve the efficiency of the UGV MCR-DWPT system.

In this section, the design requirements of the UGV MCR-DWPT compensation circuit topology are first summarized. Then, the research results are classified into various compensation topologies and parameter design methods, such as the coupling-independent type, the load-independent type, the coupling-load-independent type, and the reconfigurable type. This information is presented to provide inspiration for designing a compensation circuit topology for the MCR-DWPT system of the UGV.

3.2.1. Specifications of the Topology Design

According to the operating conditions of the UGV, the compensation circuit topology of the MCR-DWPT system is specified by the following instructions to improve the adaptability and reliability of the system:

1. Constant voltage/current output of the MCR-DWPT system.

The system should be able to provide a constant-voltage/current output that is not influenced by the load. The receiver of the MCR-DWPT system is used to charge the battery and other power storage components, while the load characteristics of these power storage components are prone to change during the charging process. By adopting a good compensation topology that realizes a constant-voltage/current output, the charging process is better controlled and the charging efficiency is improved [32].

2. Constant current output of the transmitter.

The transmitter should be able to output a load-independent constant current, in which case the current is not influenced by the changing impedance of the receiver. Subsequently, this protects the transmitting devices from an overload current in the case of an open circuit at the receiver [33].

3. Zero phase angle (ZPA) of input impedance.

During the operation of the MCR-DWPT system, the problems of large leakage inductance of the coupling device, high reactive power, and reduced efficiency of the system may occur due to the large air gap between the transmitter and the receiver device. Therefore, an appropriate compensation topology needs to be designed to keep the input voltage and current at the transmitter terminal in phase and make the input impedance of the system pure resistance, which helps to realize the input impedance to meet the ZPA condition and reduce the reactive power of the system [34].

4. Zero Voltage Switching (ZVS).

The high-frequency inverter circuit at the transmitter inverts the input DC power into high-frequency AC power, which produces switching losses and reduces the efficiency of the system at the same time. Current research makes the transmitter input impedance weakly inductive by adjusting the transmitter compensation parameters and making the voltage phase ahead of the current phase by one phase angle to achieve ZVS and reduce switching losses [35].

Considering that the operating condition is mainly desolate places, the transmitters and the receivers are in a weak coupling condition. The compensation circuit topology is essential to keep the output voltage, current, power, and efficiency of the system stable while the coupling coefficient and load conditions are changing. For the compensation circuit topologies discussed below, the default system input is a constant voltage source and the internal resistance of the device is ignored, unless otherwise specified. The frequency bifurcation phenomenon under strong coupling conditions [36] and the unilateral compensation topology with fewer application components used in low-power application scenarios [37] are not considered.

3.2.2. Topology Design of Load-Independent Compensation Circuits

The load resistance, inductive reactance, and capacitive reactance of the MCR-DWPT system change due to different operating conditions. The following section describes the MCR-DWPT system with a pure resistance load, a resistance–inductance load, and a resistance–capacitance load.

For an MCR-DWPT system with a constant pure resistive load, scholars have designed a variety of compensation circuit topologies, including the basic compensation topology, the high-order compensation topology, and the hybrid compensation topology, to achieve a system output independent of the load.

Although the four basic compensation topologies of S/S, S/P, P/S, and P/P are able to realize a constant-voltage or constant-current output independent of the load, they cannot meet the requirements of the MCR-DWPT system because of weak adaptability to mutual inductance changes [3]. The structures of the mentioned basic compensation topologies are shown in Figure 5. In the diagrams of the circuits, U_{in} is the input high-frequency AC voltage generated by the inverter. C_P and C_S are the compensating capacitors. L_1, L_2, and M are the transmitter self-inductance, receiver self-inductance, and mutual inductance of the coupling devices, respectively. R_L is the resistance of the load. The S/S-type and S/P-type compensation topologies can achieve a constant-current or constant-voltage output by adjusting the parameters, but there is a risk of overcurrent because the input impedance is only the parasitic resistance of the transmitter device under a light load or no load. An additional protection circuit is needed to prevent the system from being damaged due to an excessive offset between the transmitter and the receiver. The P/S-type and P/P-type compensation topologies are only applicable to an MCR-DWPT system whose input power supply is a current source because there is no DC blocking capacitor on the transmitter of the compensation topology, and the AC component of the input current leads to the saturation of the magnetic core in the coupling mechanism, which makes the system ineffective.
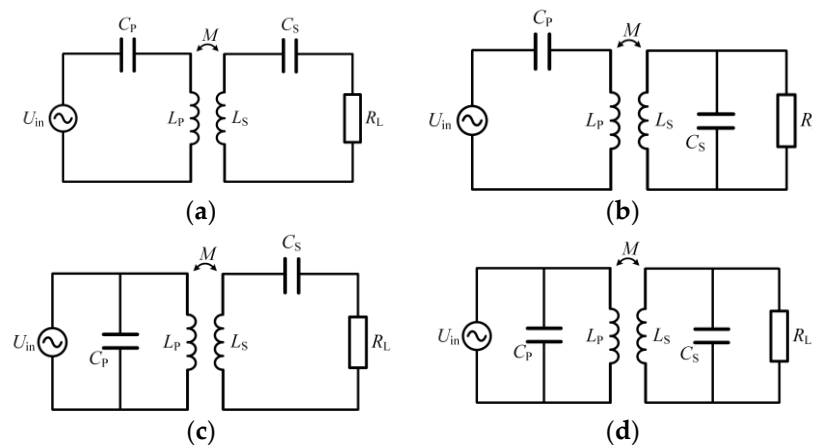
Figure 5. Four basic compensation topologies: (**a**) S/S; (**b**) S/P; (**c**) P/S; and (**d**) P/P.

The traditional high-order compensation topologies such as the LCL/LCL type and the LCC/LCC type are able to realize a load-independent constant-current output. The LCC/LCC type retains the advantage over the LCL/LCL type that the output current is independent of the load resistance and proportional to the coupling coefficient, and the system design freedom is increased. The disadvantage is that the number of compensation devices is large. In [38], an LC/S-type constant-current-output load-independent compensation circuit topology was proposed. This topology requires fewer compensation devices. However, most of the loads are voltage-type loads, so it is necessary to design a load-independent compensation circuit topology with a constant-voltage output. In [35], a novel LCC/S-type compensation topology based on a T-type resonant network was proposed. This topology has the advantages of constant gain, near-zero reactive power, the easy realization of ZVS, and high efficiency. In [39], a passive component optimization method based on an S/LCC-type compensation topology was proposed. This method is used to charge a group of electric bicycles at the same time with a high-frequency inverter. Using the optimization method, the number of components is reduced, and the optimized topology can still achieve a constant-current and a constant-voltage output. The overall cost of the system is reduced accordingly. The high-order compensation topologies mentioned above are shown in Figure 6.
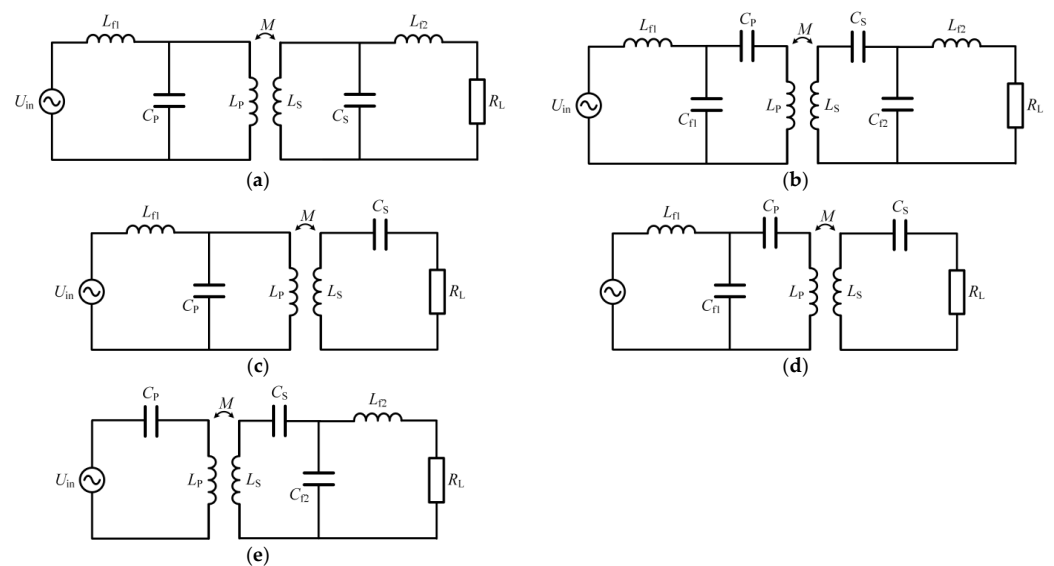
Figure 6. High-order compensation topologies: (**a**) LCL/LCL; (**b**) LCC/LCC; (**c**) LC/S; (**d**) LCC/S; and (**e**) S/LCC.

For an MCR-DWPT system with a resistance–inductance load, a resistance–capacitance load, or variable load resistance, most of the current studies use the basic compensation topology to identify the load parameters. The calculation speed and the accuracy of the load identification are low for the high-order compensation topology because of the high order of the mathematical model and the size of the calculation. In [40], for the S/S-type compensation topology, a load parameter identification method based on a genetic algorithm was proposed. The method uses the transmitter sampling data to calculate the parameters, and the system load degree is low. However, the method only estimates the load resistance. In [32], for an LCC/LCC-type compensation topology, an identification method for battery load parameters based on measured transmitter circuit parameters was proposed. This method accurately estimates a battery's state of charge.

3.2.3. Topology Design of Coupling-Independent Compensation Circuit

Due to the relative motion between the transmitter and the receiver of the MCR-DWPT system, the coupling coefficient of the system changes. The traditional way of compensating for the self-inductance or leakage inductance of the device causes the system parameters to change with the coupling coefficient, which affects the stability of the system. A variety of algorithms are used to design the parameters of the compensation capacitor and the inductance, which makes the compensation topology insensitive to changes in the coupling coefficient and improves the stability of the system. In [41], a design method for compensation topology parameters based on a particle swarm optimization (PSO) algorithm was proposed, and the parameters of an S/CLC-type compensation topology were designed. The experimental results show that the method significantly reduces the ripple voltage change in the system when the coupling coefficient and load change. In addition, the power transmission efficiency of the WPT system is improved. In [42], a multi-objective optimization method for the power fluctuation factor and the reactive power component based on a genetic algorithm (GA) was proposed, and the parameters of a T-type compensation topology were designed. The experimental results show that the method effectively reduces the power factor fluctuation caused by changes in the coupling coefficient due to changes in the device gap in the process of DWPT in electric vehicles.

3.2.4. Topology Design of Reconfigurable Compensation Circuits

In order to adapt to different working conditions, scholars have proposed a variety of reconfigurable compensation circuit topologies that adapt to various output modes by switching the topology and greatly improve the flexibility of the MCR-DWPT system.

In [43], a reconfigurable compensation circuit topology based on the receiver of the LCL-type compensation topology was proposed. The automatic switching method of the constant-current and constant-voltage charging mode is completed by switching the parameters of the receiver resonance compensation network. This method does not need wireless communication between the transmitter and the receiver and does not need to change the input voltage or frequency of the transmitter. The switching process is stable. In [44], based on the equivalent detuning S/S-type compensation topology, a reconfigurable compensation circuit topology and its parameter design method were proposed. By establishing the power-coupling coefficient (P-k) curves of two compensation topologies, the system is able to operate in the top regions of the P-k curves by switching from one topology to another, which helps to improve the system's efficiency. In [45], a reconfigurable compensation circuit topology based on a capacitor matrix was proposed. This topology is able to ensure the impedance matching of the variable frequency system by controlling the switch to dynamically connect the specific capacitor in order to realize the encryption of the DWPT system for a cluster of electric vehicles. Figure 7 shows the structures of the three reconfigurable compensation circuits mentioned above.
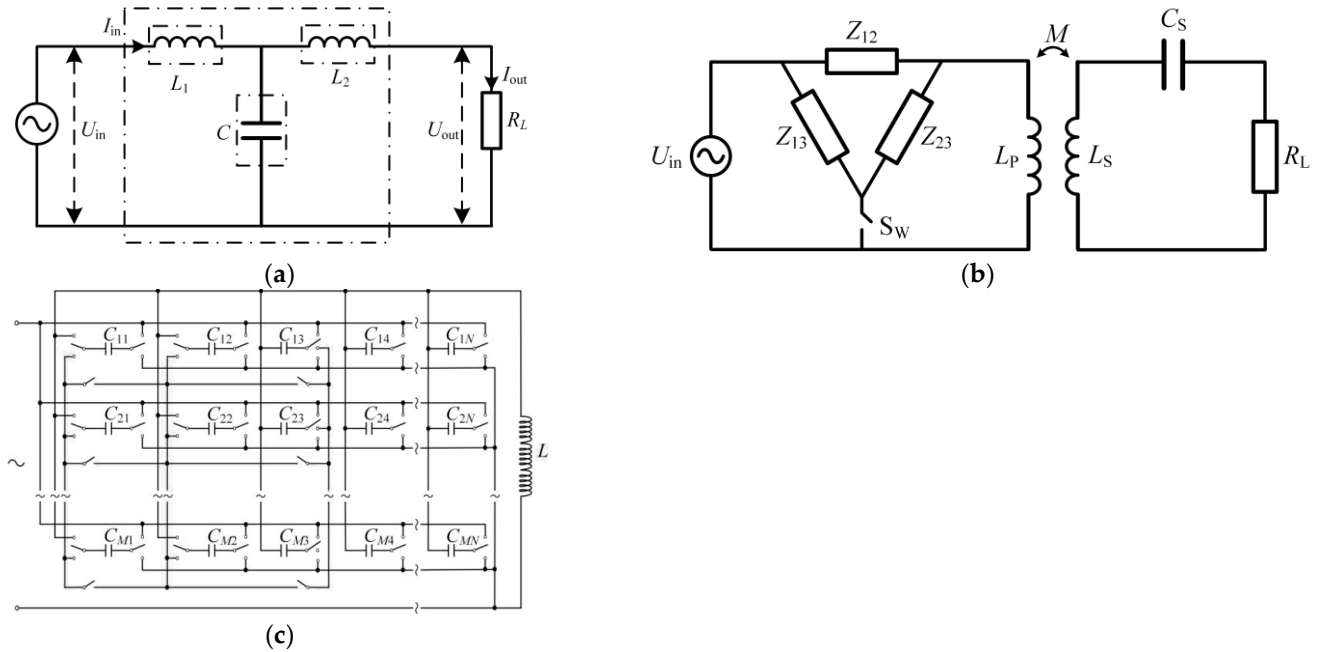
Figure 7. The structures of the three reconfigurable compensation circuits: (**a**) a reconfigurable compensation circuit topology based on the receiver of the LCL-type compensation topology; (**b**) a reconfigurable compensation circuit topology based on the equivalent detuning S/S-type compensation topology; and (**c**) a reconfigurable compensation circuit topology based on a capacitance matrix (capacitance matrix section).

3.3. Strategy Research of System Control

The control strategy of the MCR-DWPT system is to improve the transmission power or efficiency of the system on the premise of maintaining stability under dynamic conditions as well as to make the system operate quickly and stably when switching operating conditions. The MCR-DWPT system control mode can be divided into four types: transmitter control, receiver control, bilateral open-loop control, and bilateral closed-loop control [3]. Four control structures of the MCR-DWPT of UGVs are shown in Figure 8.
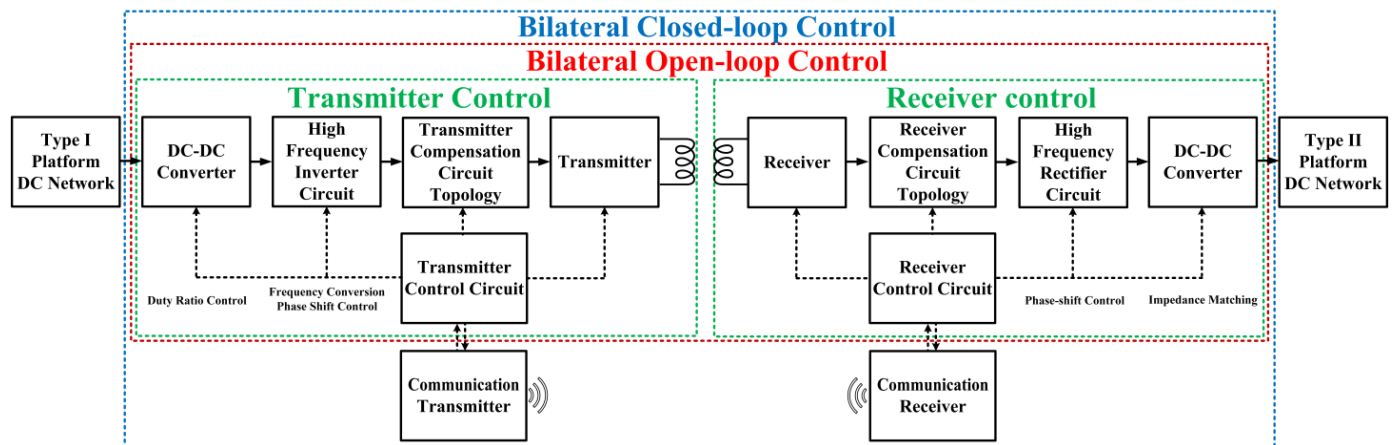
Figure 8. Control structures of MCR-DWPT of UGVs.

3.3.1. Transmitter Control

The transmitter control of the MCR-DWPT system includes the frequency conversion and the phase shift control of the high-frequency inverter as well as the duty ratio control

of the transmitter DC-DC converter. In [46], a proportional–integral (PI) controller was used to control the phase shift angle of a phase-shifted full-bridge circuit, which realized constant-voltage and constant-current control without communication with the receiver.

The transmitter-side control does not need to communicate with the receiver and rely on the load, but it is unable to adjust the load output and achieve the maximum efficiency.

3.3.2. Receiver Control

The transmitter control of the MCR-DWPT system includes the phase shift control of the high-frequency rectifier, load control, the impedance matching of the receiver DC-DC converter, and so on. In [47], a power fluctuation suppression strategy based on a buck–boost circuit was proposed for the DWPT of electric vehicles with a single transmitter and a receiver. In [48], by realizing the double-closed-loop control of an outer-loop constant-current mode and an inner-loop saturation constant-voltage mode of a DC/DC circuit on the vehicle side, the transmission efficiency of the system was improved and the high-frequency inverter on the ground side was ensured to work in a soft switching state. In [49], by establishing the state-space model of the buck circuit at the power receiver, a constant-current control method combining a Kalman filter and a model of predictive control was proposed. This method is able to significantly improve the speed of constant-current control at the receiver of the MCR-DWPT system and has strong robustness during changes in mutual inductance.

The receiver control does not require data communication with the transmitter and achieves a constant-voltage, constant-current, or maximum-efficiency output on the load side. However, the receiver cannot achieve a wide range of control due to the inability to control the parameters of the transmitter.

3.3.3. Bilateral Open-Loop Control

The bilateral open-loop control of the MCR-DWPT system controls the transmitter and the receiver without communication. The transmitter and the receiver are able to be closed-loop-controlled independently. Because there is no communication between the transmitter and the receiver, the whole system is in open-loop control. In [50], a bilateral non-communication control strategy was proposed. In this strategy, the disturbance and observation method is used to shift the phase of the inverter in the transmitter to track the system with maximum efficiency. The PI control is used to adjust the phase-shifting angle in the receiver to achieve a constant-current output.

Bilateral open-loop control is able to simultaneously achieve maximum power control in the transmitter and maximum efficiency control in the receiver. However, due to the lack of communication between the transmitter and the receiver, there are control conflicts in the system, which reduce the stability of the system.

3.3.4. Bilateral Closed-Loop Control

The bilateral closed-loop control of the MCR-DWPT system is mainly to control the transmitter and the receiver as a whole system under the condition of communication. The data exchange between the transmitter and the receiver is the premise of bilateral closed-loop control. There are three common communication modes: short-distance wireless communication, dual-channel transmission, and shared-channel transmission. According to the different types of communication modules, short-range wireless communication can be divided into Wi-Fi, ZigBee [51], Bluetooth, infrared, 4G, and 5G, etc. Dual-channel transmission is divided into the magnetic-field eccentric type [52], the magnetic-field coaxial type [53], and the electric-field type [54], according to the nature and location of the data transmission channel. The shared-channel transmission mode is divided into the amplitude-modulation type [55], the tuning type [56], the time-division multiplexing (TMD) type, and the frequency-division multiplexing (FMD) type [57], according to the different data injection methods. The advantages and disadvantages of various communication modes are shown in Table 2.

Table 2. The advantages and disadvantages of various communication modes [52–59].

Means of Communication	Classifications	Advantages	Disadvantages
Wireless communication	Wi-Fi	Wide range coverage	Vulnerable to electromagnetic interference
	ZigBee	Low power consumption	Weak communication stability
	Bluetooth	Low complexity	Short transmission distance
	Infrared Communication	Good confidentiality	Weak anti-offset ability
	4G/5G	High bandwidth and transmission rate	Requirement of communication stations
		Low transmission delay	
Dual-channel transmission	Magnetic-field eccentric type	Low crosstalk	Large volume
		High data transmission rate	Sensitive to angle offset
	Magnetic-field coaxial type	Small volume	High crosstalk
		High data transmission rate	Complicated implementation
	Electric-field type	Low crosstalk	Complex system
		High data transmission rate	Weak anti-offset ability
Shared-channel transmission	Amplitude-modulation type	Simple principle	Poor anti-noise property
		Easy implementation	High bit error rate
	Tuning type	High anti-noise property	Output power greatly affected by the operating frequency
		Full duplex data transmission	Low communication rate
	TMD type	Simple principle	Complicated control system
			Low reliability
	FMD type	High data transmission rate	Complicated design of data injection, extraction circuit, and filter circuit
		High anti-noise property	
		Easy implementation	

In [58], an optimal impedance control strategy based on an active single-phase rectifier (ASPR) was proposed. Two closed loops are applied to regulate the equivalent resistance and reactance of the ASPR to make sure that not only the receiver side is resonant but also the equivalent resistance of the load is close to the optimal one. Another closed loop is dedicated to regulating the output voltage/current by adjusting the input voltage. The measured output voltage V_0 is transferred to the transmitter-side controller via a wireless communication link. A PI controller is employed to regulate the output voltage by adjusting the pulse-width α of the inverter. In [51], a DWPT control system based on an LCC/S-type compensation topology was proposed. In this system, the duty ratio of the DC/DC converter is controlled by PI controllers in both the transmitter and the receiver, and the mutual inductance of the devices can be estimated quickly to realize a stable output and maximum-efficiency tracking under dynamic conditions. In [59], based on the LCL/S-type compensation topology, a method of dynamically searching for the optimal operating frequency related to the load was proposed. This method does not rely on the estimation of the load or the coupling coefficient. The system's efficiency can be improved by dynamically changing the pulse width of the transmitter's high-frequency inverter according to the circuit parameters of the transmitter and the receiver.

Bilateral closed-loop control is able to realize the control of multiple output modes because of the data exchange between the transmitter and the receiver, but the real-time performance of the system is poor because of the communication delay.

4. Key Challenges in MCR-DWPT of UGV

Although a large number of research achievements have been made in the field of MCR-DWPT, there are still many challenges to be investigated, which are listed as follows:

1. The anti-offset performance of the coupling device has to be improved.

At present, the proposed structure of the MCR-DWPT device on UGVs generally has the shortcomings of a complex device structure, large mass and volume, and a large ferrite

core, which increases the cost of the device and limits the application scenarios of the device. Coupling devices with resistance to horizontal offset are highly required for the carrier-type grouping of UGVs, and anti-angle-offset coupling devices are of great use to the system of the formation-type grouping of UGVs. In addition, in order to realize the "charging while driving" of the UGVs, it is necessary to design a coupling device to meet the requirements of high power and efficiency. Further studies are needed related to the aspects of the transmission power level, transmission efficiency, and electromagnetic shielding.

2.　The topology of the compensation circuit has to be optimized.

Current research on the topology of the compensation circuit is fruitful, and various compensation topologies and parameter design methods have been proposed to reduce the reactive power of the system and improve the stability of the system's output. However, due to the relative motion of UGVs, the coupling device of the transmitter and the receiver dynamically change their relative position and the working conditions often switch according to the operating situation. Therefore, the requirements for the adaptability of compensation topology parameters to changes in coupling coefficients and load characteristics continue to increase. The future research directions of compensation circuit topology will mainly focus on the optimization algorithm design of compensation circuit parameters, dynamic system modeling, reconfigurable compensation topology design, and so on.

3.　The system control strategy has to be improved.

The current research on the control strategy of the MCR-DWPT system mainly has the difficulties of poor real-time control, the low accuracy of dynamic parameter identification, the complex structures of detection and control circuits, and so on. As for both the carrier-type and the formation-type grouping of UGVs, the priority of power and efficiency is a question to be answered in the design of system control strategy. Moreover, simultaneous wireless power and data transfer for real-time control, intelligent algorithms to estimate the coupling coefficient and load characteristics of the MCR-DWPT system, and a simplified design of the control system need to be further researched to enhance the MCR-DWPT system.

In addition to the three challenges mentioned above, the MCR-DWPT system of UGVs also has many disadvantages related to electromagnetic compatibility (EMC), foreign object detection (FOD), and environmental adaptability that need to be studied further.

5. Conclusions

In this paper, the research status of the MCR-DWPT technology of UGVs is reviewed, including the aspects of the coupling device, compensation circuit topology, and system control strategy. The basic structure and characteristics of the MCR-DWPT system of UGVs are summarized, the key challenges to be investigated are reviewed, and future research directions are proposed. With the development of key technologies mentioned above, MCR-DWPT systems are increasingly applied to both the carrier-type and the formation-type groupings of UGVs in the near future. As for the carrier-type grouping of UGVs, MCR-DWPT systems are hopefully reaching short-distance (less than 50 cm) MCR-DWPT with an efficiency of more than 90 percent and an anti-offset distance of up to tens of centimeters. Moderate-distance (about one meter to several meters) MCR-DWPT with tens of kilowatts of power and an efficiency of about 70 percent has the opportunity to be realized in the formation-type groupings of UGVs. Although MCR-DWPT technology still has many issues to be advanced, as a convenient, safe, and environmentally adaptable power transmission mode, it has great research prospects in both UGVs and other industrial fields.

Author Contributions: Conceptualization, F.X. and D.Y.; methodology, S.W.; software, J.L.; validation, F.X., S.W., and J.L.; formal analysis, D.Y.; investigation, S.W.; resources, D.Y.; data curation, J.L.; writing—original draft preparation, F.X.; writing—review and editing, J.L.; visualization, F.X.; supervision, J.L.; project administration, D.Y.; funding acquisition, S.W. All authors have read and agreed to the published version of the manuscript.

Funding: This research was funded by the Industrial Bureau of China (grant number 20222020161). The APC was funded by Dong Yuan.

Data Availability Statement: This study did not include any data.

Conflicts of Interest: The authors declare no conflict of interest.

References

1. Li, J.; Wei, S.; Liao, Z.; Zang, K. Review on the development of all-electric key technologies for land warfare platforms. *J. Ordnance Eng.* **2021**, *42*, 2049–2059.
2. Ma, X.; Yuan, D.; Xiang, Y.; Wei, S. Research on integrated power system of land warfare platform and its key technologies. *J. Ordnance Eng.* **2017**, *38*, 396–406.
3. Patil, D.; McDonough, M.K.; Miller, J.M.; Fahimi, B.; Balsara, P.T. Wireless Power Transfer for Vehicular Applications: Overview and Challenges. *IEEE Trans. Transp. Electrific.* **2018**, *4*, 3–37. [CrossRef]
4. Chen, K.; Cheng, K.W.E.; Yang, Y.; Pan, J. Stability Improvement of Dynamic EV Wireless Charging System with Receiver-Side Control Considering Coupling Disturbance. *Electronics* **2021**, *10*, 1639. [CrossRef]
5. Lee, E.S.; Sohn, Y.H.; Choi, B.G.; Han, S.H.; Rim, C.T. A Modularized IPT With Magnetic Shielding for a Wide-Range Ubiquitous Wi-Power Zone. *IEEE Trans. Power Electron.* **2018**, *33*, 9669–9690. [CrossRef]
6. Dinis, H.; Mendes, P.M. A Comprehensive Review of Powering Methods Used in State-of-the-Art Miniaturized Implantable Electronic Devices. *Biosens. Bioelectron.* **2021**, *172*, 112781. [CrossRef]
7. La Rosa, R.; Livreri, P.; Trigona, C.; Di Donato, L.; Sorbello, G. Strategies and Techniques for Powering Wireless Sensor Nodes through Energy Harvesting and Wireless Power Transfer. *Sensors* **2019**, *19*, 2660. [CrossRef]
8. Li, Y.; Ni, X.; Liu, J.; Wang, R.; Ma, J.; Zhai, Y.; Huang, Y. Design and Optimization of Coupling Coils for Bidirectional Wireless Charging System of Unmanned Aerial Vehicle. *Electronics* **2020**, *9*, 1964. [CrossRef]
9. Afonso, J.A.; Duarte, H.G.; Cardoso, L.A.L.; Monteiro, V.; Afonso, J.L. Wireless Communication and Management System for E-Bike Dynamic Inductive Power Transfer Lanes. *Electronics* **2020**, *9*, 1485. [CrossRef]
10. Shi, K.; Tang, C.; Long, H.; Lv, X.; Wang, Z.; Li, X. Power Fluctuation Suppression Method for EV Dynamic Wireless Charging System Based on Integrated Magnetic Coupler. *IEEE Trans. Power Electron.* **2022**, *37*, 1118–1131. [CrossRef]
11. Mohsan, S.A.H.; Othman, N.Q.H.; Khan, M.A.; Amjad, H.; Żywiołek, J. A Comprehensive Review of Micro UAV Charging Techniques. *Micromachines* **2022**, *13*, 977. [CrossRef]
12. Zakerian, A.; Vaez-Zadeh, S.; Babaki, A. A Dynamic WPT System with High Efficiency and High Power Factor for Electric Vehicles. *IEEE Trans. Power Electron.* **2020**, *35*, 6732–6740. [CrossRef]
13. Wu, J.; Dai, X.; Sun, Y.; Li, Y. A Node Role Dynamic Change Method Among Repeater, Receiver, and Decoupling Using Topology Switching in Multinode WPT System. *IEEE Trans. Power Electron.* **2021**, *36*, 11174–11182. [CrossRef]
14. Kim, J.H.; Choi, B.G.; Jeong, S.Y.; Han, S.H.; Kim, H.R.; Rim, C.T.; Kim, Y.-S. Plane-type Receiving Coil with Minimum Number of Coils for Omnidirectional Wireless Power Transfer. *IEEE Trans. Power Electron.* **2019**, *35*, 6165–6174. [CrossRef]
15. Han, W.; Chau, K.T.; Jiang, C.; Liu, W.; Lam, W.H. Design and Analysis of Quasi-Omnidirectional Dynamic Wireless Power Transfer for Fly-and-Charge. *IEEE Trans. Magn.* **2019**, *55*, 1–9. [CrossRef]
16. Budhia, M.; Covic, G.A.; Boys, J.T. Design and Optimization of Circular Magnetic Structures for Lumped Inductive Power Transfer Systems. *IEEE Trans. Power Electron.* **2011**, *26*, 3096–3108. [CrossRef]
17. Tian, X.; Chau, K.T.; Liu, W.; Lee, C.H.T. Analysis of Multi-Coil Omnidirectional Energy Harvester. *IEEE Trans. Magn.* **2020**, *57*, 1–6. [CrossRef]
18. Cheng, W.; Jiang, B.; Zhang, K.; Ding, S.X. Robust Finite-Time Cooperative Formation Control of UGV-UAV with Model Uncertainties and Actuator Faults. *J. Frankl. Inst.* **2021**, *358*, 8811–8837. [CrossRef]
19. Budhia, M.; Boys, J.T.; Covic, G.A.; Huang, C.-Y. Development of a Single-Sided Flux Magnetic Coupler for Electric Vehicle IPT Charging Systems. *IEEE Trans. Ind. Electron.* **2013**, *60*, 318–328. [CrossRef]
20. Zaheer, A.; Kacprzak, D.; Covic, G.A. A Bipolar Receiver Pad in a Lumped IPT System for Electric Vehicle Charging Applications. In Proceedings of the 2012 IEEE Energy Conversion Congress and Exposition (ECCE), Raleigh, NC, USA, 15–20 September 2012; pp. 283–290.
21. Nagendra, G.R.; Covic, G.A.; Boys, J.T. Determining the Physical Size of Inductive Couplers for IPT EV Systems. In Proceedings of the 2014 IEEE Applied Power Electronics Conference and Exposition-APEC 2014, Fort Worth, TX, USA, 16–20 March 2014; pp. 3443–3450.
22. Lee, S.; Huh, J.; Park, C.; Choi, N.S.; Cho, G.H.; Rim, C.T. On-Line Electric Vehicle Using Inductive Power Transfer System. In Proceedings of the 2010 IEEE Energy Conversion Congress and Exposition, Atlanta, GA, USA, 12–16 September 2010; pp. 1598–1601.
23. Huh, J.; Lee, S.W.; Lee, W.Y.; Cho, G.H.; Rim, C.T. Narrow-Width Inductive Power Transfer System for Online Electrical Vehicles. *IEEE Trans. Power Electron.* **2011**, *26*, 14. [CrossRef]
24. Choi, S.Y.; Jeong, S.Y.; Gu, B.W.; Lim, G.C.; Rim, C.T. Ultraslim S-Type Power Supply Rails for Roadway-Powered Electric Vehicles. *IEEE Trans. Power Electron.* **2015**, *30*, 6456–6468. [CrossRef]
25. Park, C.; Lee, S.; Jeong, S.Y.; Cho, G.-H.; Rim, C.T. Uniform Power I-type Inductive Power Transfer System with DQ-Power Supply Rails for On-Line Electric Vehicles. *IEEE Trans. Power Electron.* **2015**, *30*, 6446–6455. [CrossRef]

26. Nagendra, G.R.; Covic, G.A.; Boys, J.T. Sizing of Inductive Power Pads for Dynamic Charging of EVs on IPT Highways. *IEEE Trans. Transp. Electrific.* **2017**, *3*, 405–417. [CrossRef]

27. Kadem, K.; Bensetti, M.; Le Bihan, Y.; Labouré, E.; Debbou, M. Optimal Coupler Topology for Dynamic Wireless Power Transfer for Electric Vehicle. *Energies* **2021**, *14*, 3983. [CrossRef]

28. Liu, C.; Wei, B.; Wu, X.; Wang, S.; Xu, J. Engineering Application of Dynamic Wireless Charging Technology for Electric Vehicles. *Power Syst. Technol.* **2019**, *43*, 2211–2218.

29. Tan, L.; Zhao, W.; Liu, H.; Li, J.; Huang, X. Design and Optimization of Ground-Side Power Transmitting Coil Parameters for EV Dynamic Wireless Charging System. *IEEE Access* **2020**, *8*, 74595–74604. [CrossRef]

30. Zhu, Q.; Su, M.; Sun, Y.; Tang, W.; Hu, A.P. Field Orientation Based on Current Amplitude and Phase Angle Control for Wireless Power Transfer. *IEEE Trans. Ind. Electron.* **2018**, *65*, 4758–4770. [CrossRef]

31. Choi, B.G.; Sohn, Y.-H.; Lee, E.S.; Han, S.H.; Kim, H.R.; Rim, C.T. Coreless Transmitting Coils with Conductive Magnetic Shield for Wide-Range Ubiquitous IPT. *IEEE Trans. Power Electron.* **2019**, *34*, 2539–2552. [CrossRef]

32. Guo, Y.; Zhang, Y.; Zhang, W.; Wang, L. Battery Parameter Identification Based on Wireless Power Transfer System with Rectifier Load. *IEEE Trans. Ind. Electron.* **2021**, *68*, 6893–6904. [CrossRef]

33. Li, Z.; Song, K.; Jiang, J.; Zhu, C. Constant Current Charging and Maximum Efficiency Tracking Control Scheme for Supercapacitor Wireless Charging. *IEEE Trans. Power Electron.* **2018**, *33*, 9088–9100. [CrossRef]

34. Mai, R.; Zhang, Y.; Dai, R.; Chen, Y.; He, Z.A. Three-Coil Inductively Power Transfer System with Constant Voltage Output. *Energies* **2018**, *11*, 673. [CrossRef]

35. Wang, Y.; Wang, H.; Liang, T.; Zhang, X.; Xu, D.; Cai, L. Analysis and Design of an LCC/S Compensated Resonant Converter for Inductively Coupled Power Transfer. In Proceedings of the 2017 IEEE Transportation Electrification Conference and Expo, Asia-Pacific (ITEC Asia-Pacific), Harbin, China, 7–10 August 2017; pp. 1–5.

36. Sample, A.P.; Meyer, D.A.; Smith, J.R. Analysis, Experimental Results, and Range Adaptation of Magnetically Coupled Resonators for Wireless Power Transfer. *IEEE Trans. Ind. Electron.* **2011**, *58*, 544–554. [CrossRef]

37. Zhang, Y.; Yan, Z.; Liang, Z.; Li, S.; Mi, C.C. A High-Power Wireless Charging System Using LCL-N Topology to Achieve a Compact and Low-Cost Receiver. *IEEE Trans. Power Electron.* **2020**, *35*, 131–137. [CrossRef]

38. Wang, Y.; Yao, Y.; Liu, X.; Xu, D.; Cai, L. An LC/S Compensation Topology and Coil Design Technique for Wireless Power Transfer. *IEEE Trans. Power Electron.* **2018**, *33*, 2007–2025. [CrossRef]

39. Mai, R.; Chen, Y.; Zhang, Y.; Yang, N.; Cao, G.; He, Z. Optimization of the Passive Components for an S-LCC Topology-Based WPT System for Charging Massive Electric Bicycles. *IEEE Trans. Ind. Electron.* **2018**, *65*, 5497–5508. [CrossRef]

40. Su, Y.; Chen, L.; Wu, X.; Qing, X.; Tang, C. Load and Mutual Inductance Identification Method of SS-Type Magnetically-Coupled WPT System Based on Genetic Algorithm. *Trans. China Electrotech. Soc.* **2018**, *33*, 4199–4206.

41. Yao, Y.; Wang, Y.; Liu, X.; Pei, Y.; Xu, D.; Liu, X. Particle Swarm Optimization-Based Parameter Design Method for S/CLC-Compensated IPT Systems Featuring High Tolerance to Misalignment and Load Variation. *IEEE Trans. Power Electron.* **2019**, *34*, 5268–5282. [CrossRef]

42. Li, S.; Wang, L.; Guo, Y.; Tao, C.; Ji, L. Power Stabilization with Double Transmitting Coils and T-Type Compensation Network for Dynamic Wireless Charging of EV. *IEEE J. Emerg. Sel. Topics Power Electron.* **2020**, *8*, 1801–1812. [CrossRef]

43. Ji, L.; Wang, L.; Liao, C.; Li, S. Research and Design of Automatic Alteration between Constant Current Mode and Constant Voltage Mode at the Secondary Side Based on LCL Compensation Network in Wireless Power Transfer Systems. *Trans. China Electrotech. Soc.* **2018**, *33*, 34–40.

44. Chen, Y.; Yang, B.; Li, Q.; Feng, H.; Zhou, X.; He, Z.; Mai, R. Reconfigurable Topology for IPT System Maintaining Stable Transmission Power Over Large Coupling Variation. *IEEE Trans. Power Electron.* **2020**, *35*, 4915–4924. [CrossRef]

45. Zhang, Z.; Ai, W.; Liang, Z.; Wang, J. Topology-Reconfigurable Capacitor Matrix for Encrypted Dynamic Wireless Charging of Electric Vehicles. *IEEE Trans. Veh. Technol.* **2018**, *67*, 9284–9293. [CrossRef]

46. Song, K.; Li, Z.; Jiang, J.; Zhu, C. Constant Current/Voltage Charging Operation for Series-Series and Series-Parallel Compensated Wireless Power Transfer Systems Employing Primary-Side Controller. *IEEE Trans. Power Electron.* **2017**, *33*, 8065–8080. [CrossRef]

47. Zhang, M.; Tan, L.; Li, J.; Huang, X. The Charging Control and Efficiency Optimization Strategy for WPT System Based on Secondary Side Controllable Rectifier. *IEEE Access* **2020**, *8*, 127993–128004. [CrossRef]

48. Qian, H.; Zhang, L.; Chen, Q.; Quan, S. Research on Soft Switching and Control Strategy of Dynamic Wireless Charging. *Power Electron.* **2019**, *53*, 90–93+106.

49. Tian, Y.; Feng, Y.; Tian, J.; Xiang, L. Model Predictive Control for Output Current of Electric Vehicle Dynamic Wireless Charging Systems. *Trans. China Electrotech. Soc.* **2022**, *12*, 1–14.

50. Yeo, T.-D.; Kwon, D.; Khang, S.-T.; Yu, J.-W. Design of Maximum Efficiency Tracking Control Scheme for Closed-Loop Wireless Power Charging System Employing Series Resonant Tank. *IEEE Trans. Power Electron.* **2017**, *32*, 471–478. [CrossRef]

51. Mai, R.; Liu, Y.; Li, Y.; Yue, P.; Cao, G.; He, Z. An Active-Rectifier-Based Maximum Efficiency Tracking Method Using an Additional Measurement Coil for Wireless Power Transfer. *IEEE Trans. Power Electron.* **2018**, *33*, 716–728. [CrossRef]

52. He, H.; Wang, S.; Liu, Y.; Jiang, C.; Wu, X.; Wei, B.; Jiang, B. Maximum Efficiency Tracking for Dynamic WPT System Based on Optimal Input Voltage Matching. *IEEE Access* **2020**, *8*, 215224–215234. [CrossRef]

53. Babaki, A.; Vaez-Zadeh, S.; Zakerian, A.; Covic, G.A. Variable-Frequency Retuned WPT System for Power Transfer and Efficiency Improvement in Dynamic EV Charging with Fixed Voltage Characteristic. *IEEE Trans. Energy Convers.* **2021**, *36*, 2141–2151. [CrossRef]

54. Zhu, J.; Tao, B. Simultaneous Wireless Power and Data Transmission over One Pair of Coils for Sensor-Integrated Rotating Cutter. *IEEE Access* **2020**, *8*, 156954–156963. [CrossRef]
55. Liang, S.; Fang, Y. Analysis of Inductance Calculation of Coaxial Circular Coils with Rectangular Cross Section Using Inverse Hyperbolic Functions. *IEEE Trans. Appl. Supercond.* **2015**, *25*, 1–9. [CrossRef]
56. Li, X.; Tang, C.; Dai, X.; Deng, P.; Su, Y. An Inductive and Capacitive Combined Parallel Transmission of Power and Data for Wireless Power Transfer Systems. *IEEE Trans. Power Electron.* **2018**, *33*, 4980–4991. [CrossRef]
57. Fan, Y.; Sun, Y.; Dai, X.; Zuo, Z.; You, A. Simultaneous Wireless Power Transfer and Full-Duplex Communication with a Single Coupling Interface. *IEEE Trans. Power Electron.* **2021**, *36*, 6313–6322. [CrossRef]
58. Nag, S.; Koruprolu, A.; Saikh, S.M.; Erfani, R.; Mohseni, P. Auto-Resonant Tuning for Capacitive Power and Data Telemetry Using Flexible Patches. *IEEE Trans. Circuits Syst. II* **2020**, *67*, 1804–1808. [CrossRef]
59. Ji, L.; Wang, L.; Liao, C.; Li, S. Simultaneous Wireless Power and Bidirectional Information Transmission with a Single-Coil, Dual-Resonant Structure. *IEEE Trans. Ind. Electron.* **2019**, *66*, 4013–4022. [CrossRef]